

KAWASAKI STEEL TECHNICAL REPORT

No.15 (October 1986)

Manufacture of Forged Shell Rings for PWR Nuclear Reactor Vessels

Kazuo Aso, Naoyuki Abe, Kenji Saito, Kyoji Nakanishi, Akihiko Namba, Minoru Yao

Synopsis :

A 250 ton hollow ingot was made for an experimental purposes of which internal properties can be simulated to those of large-sized hollow ingots. The investigation results indicated that this ingot had less C segregation and good cleanliness. Forged shell ring, a component of the 1300 MWe PWR type nuclear reactor vessel, was manufactured from large hollow ingot by using 6000 and 4400 t forging presses, large heat treating furnace and large turn miller. Mechanical properties obtained after heat treatment showed good results. Forged shell ring turned out free of defects as the results of UT and MT which were performed by automatic UT and MT equipments. Furthermore, by using solidification simulation techniques, Kawasaki Steel is manufacturing large hollow ingots up to 320 t for forged shell rings.

(c)JFE Steel Corporation, 2003

The body can be viewed from the next page.

Manufacture of Forged Shell Rings for PWR Nuclear Reactor Vessels*



Kazuo Aso
Manager,
Shape Sec., Shape &
Bar Rolling Dept.
Mizushima Works



Naoyuki Abe
Manager,
Forging Sec.,
Plate Rolling, Casting
& Forging Dept.,
Mizushima Works



Kenji Saito
Senior Researcher,
Laboratory I,
Mizushima Research
Dept., I & S
Research Labs.



Kyoji Nakanishi
Dr. Engi.,
General Manager,
Process Research
Dept., I & S
Research Labs.



Akihiko Namba
Senior Researcher,
Steelmaking Lab.,
Process Research
Dept., I & S
Research Labs.



Minoru Yao
Senior Researcher,
Steelmaking Lab.,
Process Research
Dept., I & S
Research Labs.

1 Introduction

Most of the power reactors used in Japan are light-water nuclear reactors of either the BWR or PWR type. At present, 28 power reactors are in operation, generating power which accounts for about 20% of the total electric power production in Japan. In foreign countries, 324 nuclear power reactors are in operation, and the number appears to increase in the future.

With power demand increasing, the trend has been toward construction of larger reactor pressure vessels and a shift to the use of forgings as material from the standpoints of generation cost reduction and in-service

Synopsis:

A 250 ton hollow ingot was made for an experimental purposes of which internal properties can be simulated to those of large-sized hollow ingots. The investigation results indicated that this ingot had less C segregation and good cleanliness. Forged shell ring, a component of the 1 300 MWe PWR type nuclear reactor vessel, was manufactured from large hollow ingot by using 6 000 and 4 400 t forging presses, large heat treating furnace and large turn miller. Mechanical properties obtained after heat treatment showed good results. Forged shell ring turned out free of defects as the results of UT and MT which were performed by automatic UT and MT equipments. Furthermore, by using solidification simulation techniques, Kawasaki Steel is manufacturing large hollow ingots up to 320 t for forged shell rings.

inspection.^{1,2)} Forgings are used in the shell ring, head dome, etc. of reactor pressure vessels. In Japan, the first application of a forged shell ring in a PWR was the No. 2 Tsuruga reactor of the Japan Atomic Power Company and, in a BWR, at the No. 5 unit of the Kashiwazaki-Kariwa Nuclear Power Station of Tokyo Electric Power Co., Inc. The use of forgings in reactor pressure vessels is expected to increase in the future.

Kawasaki Steel has recently manufactured a forged shell ring for a 1 300 MWe class PWR type reactor for export by the Basic Oxygen Furnace (BOF)-RH-hollow ingot process. This report describes results of an cross sectional investigation of hollow ingots aimed at increasing the ingot size and of the manufacture of the forged shell ring for the reactor pressure vessel.

2 Cross Sectional Investigation of 250-t Hollow Ingots

To ascertain the internal quality of hollow ingots, 20- to 200-t ingots have previously been subjected to cross sectional investigations.³⁻⁵⁾ Numerous high-quality hollow ingots have been manufactured based on the results of these investigations. Hollow ingots, which feature low

* Originally published in *Kawasaki Steel Giho*, 18(1986)1, pp. 30-37

3 Manufacture of Forged Shell Ring for PWR Reactor Pressure Vessel

Mn-Ni-Mo steels are used as the material for reactor pressure vessels. These steels have tensile strength of about 60 kgf/mm² and excellent toughness. In the 1 300 MWe class, the wall thickness of the vessel is as thick as 290 mm, requiring steels excellent in homogeneity, isotropy, and weldability. The forged shell ring manufacturing process is shown in Fig. 2. BOF steel with few tramp elements was used. A 220-t hollow ingot featuring slight segregation and a clean internal surface was used in consideration of the above-mentioned results of the examination of the 250-t hollow ingot. In the forging process, a 4 400-t press was used, in combination with a 6 000-t press, in order to reduce the excess metal in forging by pressing in a stroke along the longitudinal direction.

3.1 Steelmaking

The manufacturing process of the 200-t hollow ingot for a forged shell ring is schematically shown in Fig. 3.⁶⁾ After the reduction of the sulfur content to 0.003% or less by torpedo car desulfurization and ladle desulfurization, the hot metal from the blast furnace is charged into the basic oxygen furnace, where the primary refining is conducted. The phosphorous content of the hot metal is reduced to about 0.020% by this primary refining. In recent years, it has become possible to easily lower the phosphorous content through not

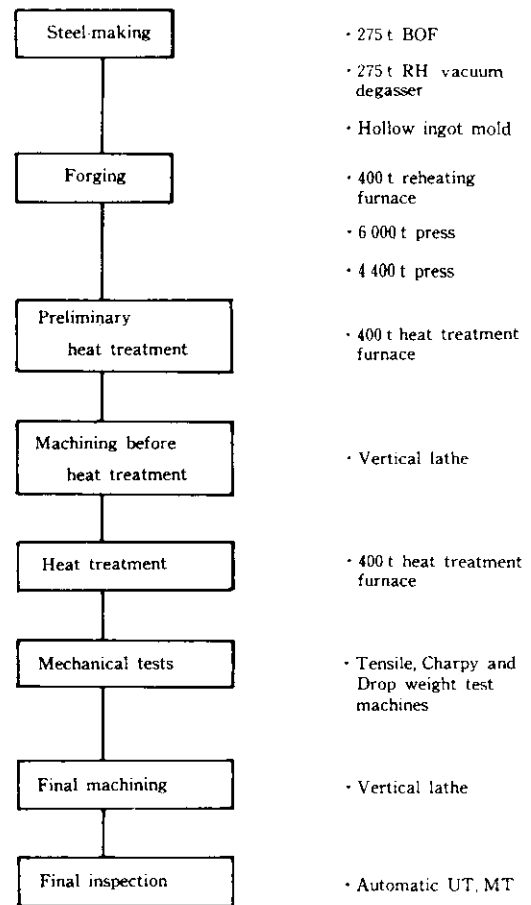


Fig. 2 Manufacturing process of forged shell ring

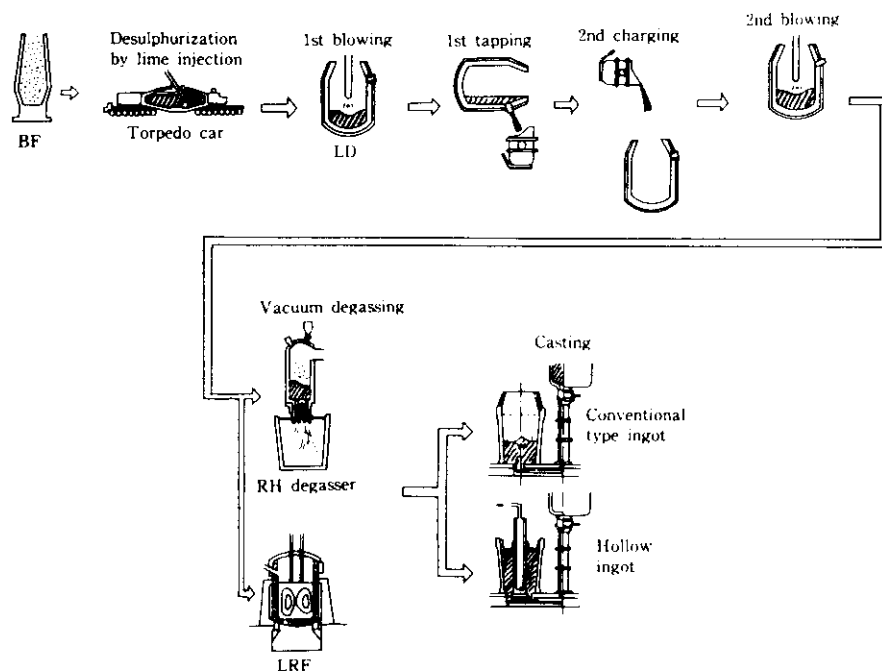


Fig. 3 Steelmaking process of high quality forging ingots

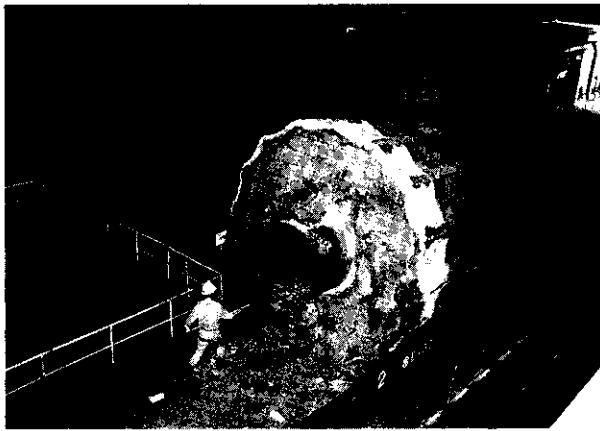


Photo 2 220 t hollow ingot



Photo 3 Forging process by 4400-t press

only the above-mentioned hot metal desulfurization but the establishment of hot metal dephosphorizing techniques. Subsequently, decarburization, dephosphorization, and heating are conducted during secondary refining. After the completion of the blowing, alloying elements are added when tapping the molten steel into the ladle. The final adjustment of the chemical composition is conducted during RH degassing. Through these steps, $P \leq 0.006\%$, $S \leq 0.003\%$, $O \leq 20$ ppm, and $H \leq 1.5$ ppm can be ensured. When this process is adopted, tramp elements of basic oxygen furnace steel are smaller in quantity than those of electric-furnace steel; $Cu \leq 0.02\%$, $As \leq 0.004\%$, $Sn \leq 0.002\%$, $Sb \leq 0.0005\%$, and $Co \leq 0.005\%$ can be ensured.

The molten steel thus obtained is poured into a 220-t hollow ingot mold by the argon-sealed bottom casting method. The appearance of the 220-t hollow ingot is shown in **Photo 2**; the ladle analysis of the steel is given in **Table 2**. This composition shows the advantages of basic oxygen furnace steel, with its very low contents of phosphorous, sulfur and tramp element.

3.2 Forging

A forging produced by a 4 400-t press is shown in **Photo 3**. Rough forging was conducted by a 6 000-t press, and finish forging by the 4 400-t press.⁷⁾ This 4 400-t press is a new press comprising a side housing, a head, and a slide beam equivalent to the cross head. This is a unique press applied to the finish forging of large-diameter shell rings and the forging of super-wide forged

plates (maximum width, 7.5 m). Since the full length of the ingot can be reduced in thickness by the slide beam, the finishing allowance in the longitudinal direction can be made uniform and it is possible to reduce the extra thickness allowed for machining. Furthermore, an outside diameter measuring device using a laser range finder is provided for three-dimensional measurement of the shape of the ring. This device makes possible measurement of ring outside diameter in any position with accuracy of ± 5 mm.

3.3 Heat Treatment

The forged shell ring was water quenched after 9-h holding at 880°C and air cooled after 9-h holding at 640°C. Each temperature was controlled by thermocouples attached to the shell ring. The heat treating furnace is of the gas combustion car-bottom type 10 m in width, 6 m in height, and 14 m in length, and is capable of loading a total of 400 t. Ceramic fiber is used in the roof to save energy and ensure uniform temperature distribution. The accuracy of the furnace temperature control is within $\pm 10^\circ\text{C}$ relative to the target temperature. The quenching water bath is 8.5 m in effective diameter and 6.7 m in depth, and performs forced stirring by propellers placed in the center and around the circumference of the bath and by spray cooling from the inside the bath. In addition, a refrigeration unit and a 1 000-t reserve water tank are provided to prevent any increase in the water temperature during cooling for

Table 2 Chemical analysis

	C	Si	Mn	P	S	Ni	Cr	Mo	Cu	V	Al	Co	Nb	B	As	Sn	Sb	H(ppm)
Specification	≤ 0.20	0.10 ~0.30	1.15 ~1.55	≤ 0.015	≤ 0.012	0.50 ~0.80	≤ 0.25	0.45 ~0.55	≤ 0.20	≤ 0.01	≤ 0.04	≤ 0.03	—	—	—	—	—	≤ 1.5
Ladle analysis	0.17	0.25	1.44	0.004	0.002	0.75	0.20	0.51	0.01	0.004	0.016	0.004	0.001	0.0001	0.001	0.001	0.0004	0.9

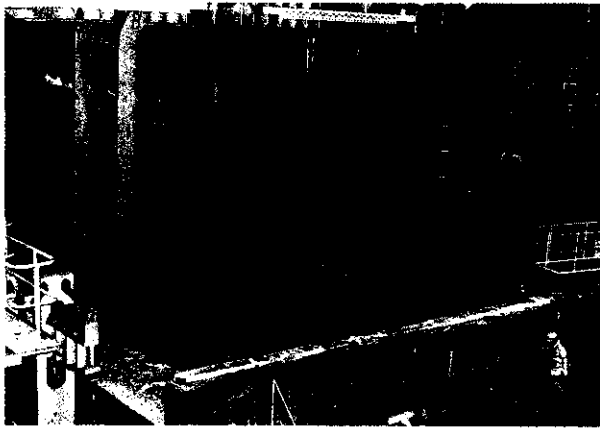


Photo 4 Heat treatment of forged shell ring

hardening. The hardening condition of the forged shell ring is shown in **Photo 4**.

3.4 Machining

Forged shell rings are machined before heat treatment to ensure uniform heat treatment. After the quality heat treatment and mechanical tests, forged shell rings are machined to the finish shape. The large turn miller, installed to machine these large forged shell rings, is a composite type vertical lathe in the top size class in the world and of the latest design. With the functions of both a vertical lathe and a gantry miller, its gantry can move up to 10 m in the front-to-back direction. Provided with an NC control, this turn miller can

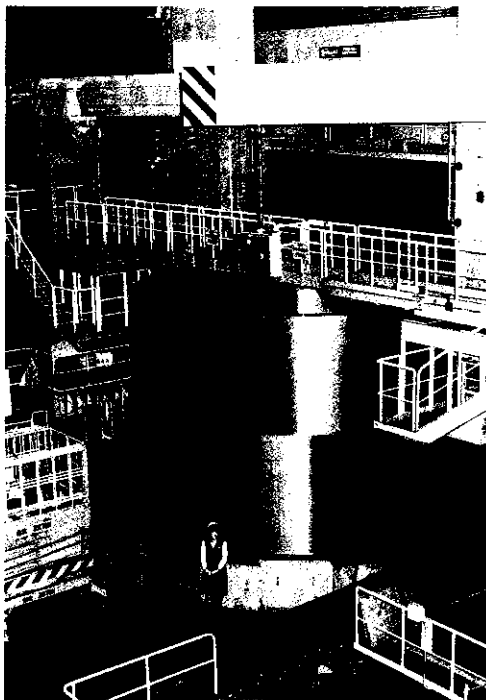


Photo 5 Large turn miller

perform three-dimensional machining of curved surfaces and has wide application, ranging from super-heavy machining to finish machining. The basic specifications of this turn miller are shown below.

- Maximum diameter of work: 9 000 mm
- Maximum height of work: 5 000 mm
- Maximum weight of work: 250 t
- Gantry stroke: 10 000 mm
- Table diameter: 8 000 mm

An example of machining with this large turn miller is shown in **Photo 5**.

3.5 Mechanical Tests

To ascertain whether the specified strength and toughness were obtained in the heat treatment, specimens were cut from the portions of the forged shell ring corresponding to the top and bottom of the ingot and from the portions of the shell ring removed for nozzle openings; sampling positions are shown in **Fig. 4**. Mechanical test results on these specimens are shown, along with required values, in **Table 3**. All of the characteristics of the steel met requirements, and differences between top and bottom were small. Thus, the homogeneity of this product can be judged to be excellent.

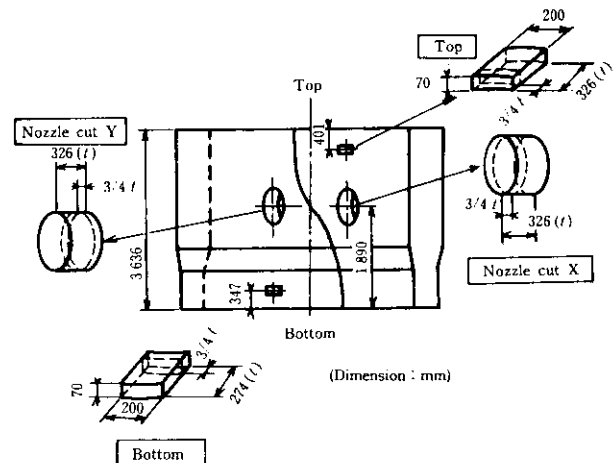


Fig. 4 Sampling position for mechanical tests

3.6 Fracture Toughness Test

The fracture toughness test was conducted using the 25-mm CT specimen shown in **Fig. 5**. Specimens were taken from the 1/4 and 3/4 thicknesses parallel to the main forging direction. A fatigue crack was formed under the condition that the stress intensity factor $K_{f \max}$ does not exceed 70 kgf/mm². The side groove was machined after the fatigue crack was formed. The load vs. load line displacement curve was recorded during the test, J_{IC} was measured by the unloading compliance method specified in ASTM E813, and $K(J_{IC})$ was calcu-

Table 3 Mechanical properties

		TS (MPa)	YS (MPa)	El (%)	RA (%)	Absorbed energy*1 (daj/cm ²)						RT _{NDT} (°C)			
						20°C			0°C				-20°C		
Specification		550/670	≥400	≥20	—	≥11.0			≥9.0			≥7.0			≤0
After Q-T, tangential, 3/4 t	Top	627	489	22	67	28.9	28.0	30.4	28.5	21.8	26.8	21.8	17.2	21.4	
	Nozzle cut out "X"	630	478	24	73	27.1	26.3	26.3	23.4	28.4	27.4	20.8	21.0	20.3	
	Nozzle cut out "Y"	627	482	25	72	28.4	28.4	27.4	29.4	25.9	30.3	22.4	23.3	21.7	
	Bottom	584	456	25	66	32.7	31.5	32.6	29.5	33.6	29.5	19.5	20.0	24.6	
After PWHT, tangential, 3/4 t	Nozzle cut out "X"	620	473	25	73				23.4	21.9	21.1				≤ -12

*1 Charpy impact test: Axial direction

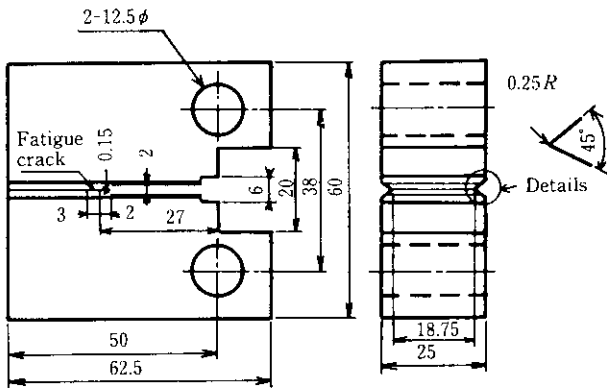


Fig. 5 1 TCT specimen-geometry (mm)

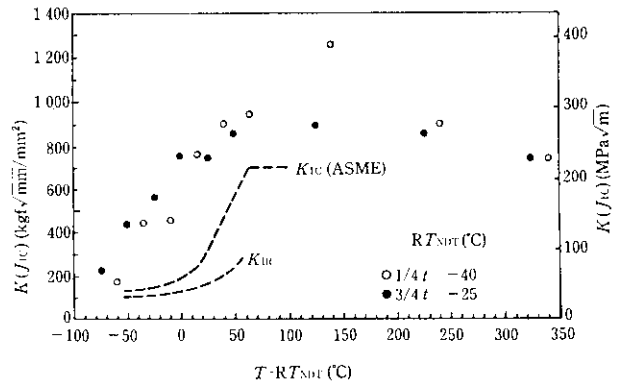


Fig. 6 Plot of $K(J_{1C})$ vs. $T-RT_{NDT}$

lated by Eq. (1).

$$K(J_{1C}) = \sqrt{EJ_{1C}/(1 - \nu^2)} \dots \dots \dots (1)$$

where E : Elastic modulus
 ν : Poisson's ratio

Results of the fracture toughness test are shown in Fig. 6. The K_{IC} curve and K_{IR} curve specified in ASME code are also plotted in the figure. The obtained results were well within standard, and the difference between the specimens taken at 1/4 and 3/4 thicknesses was small.

3.7 Nondestructure Inspection

The appearance of the finished forged shell ring is shown in Photo 6. Ultrasonic inspection and magnetic particle inspection were conducted as nondestructive tests of the finished product.

Automatic equipment was employed for both ultrasonic inspection and magnetic particle inspection.⁸⁾ Photo 7 shows the general view of the automatic ultra-



Photo 6 Forged shell ring produced by 220-t hollow ingot

sonic inspection equipment employed. The spiral continuous scanning method was used. The specifications of this equipment are as follows:

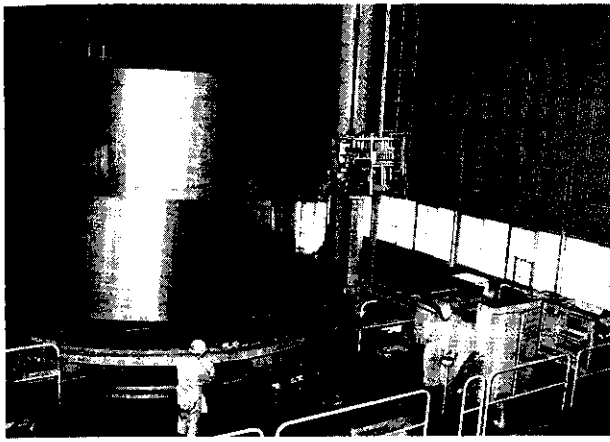


Photo 7 Automatic ultrasonic equipment for large forged shell ring

Maximum weight of work: 200t
 Maximum outside diameter: 7.5 m
 Maximum height: 5 m
 Turning speed: 0 to 0.888 rpm (infinitely variable)
 Peripheral speed: 0 to 150 mm/s (outside diameter, 3.5 m)

The probe head is composed of six channels and can be employed as a double spiral head or single spiral head. The probe head is kept in direct contact with a thin film of couplant using a probe shoe. Results of flaw detection are output by printer. When a defect is detected, the portion in question is reexamined by manual detection using a general-purpose flaw detector, and the defect is evaluated based on results of this reexamination. By adopting such automatic inspection equipment, it has become possible to efficiently conduct nondestructive inspection. In this forged shell ring, no defects were detected in either ultrasonic inspection or magnetic particle inspection by the automatic equipment.

4 Discussion

4.1 Evaluation of Homogeneity of Hollow Ingot

Hollow ingots are characterized by the fact that their segregation is small and their internal surfaces are clean compared to solid ingots of the same size. As is apparent from the results of the examination of the 250-t hollow ingot, the segregation of elements, represented by carbon, is very small. Figure 7 shows the carbon content of the 220-t hollow ingot in the section just under the hot top. Samples were taken by a 7-mm ϕ drill at 20-mm intervals. The carbon content in this check analysis was a maximum 0.19% compared to the 0.17% of ladle analysis. Thus, the microsegregation of carbon was very small in spite of the large size of the 220-t ingot.

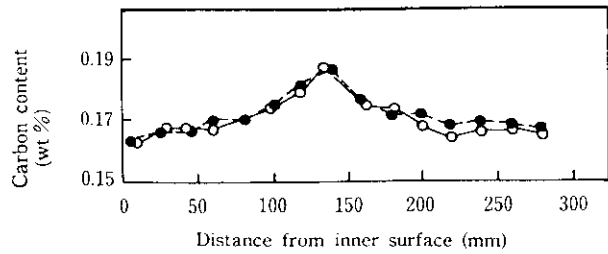


Fig. 7 Carbon distribution of forged shell ring made from 220 t hollow ingot (top sample-corresponding to top of the ingot)

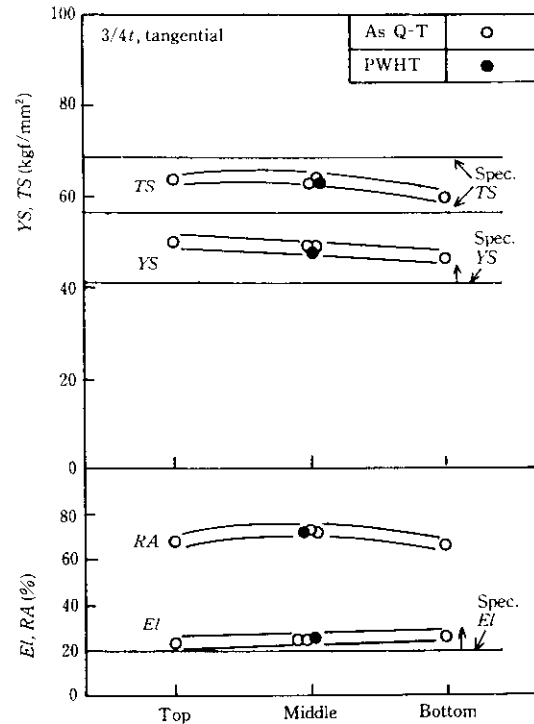


Fig. 8 Distribution of mechanical properties

To determine the relationship between this segregation and mechanical properties, an investigation was made into the relationship between positions in the ingot and the mechanical properties. The relationship between tensile strength and position in the ingot is shown in Fig. 8. Since segregation was small, the difference among positions in the ingot was also very small. Changes in properties due to difference in direction are also an important factor from the standpoint of homogeneity. Therefore, the tensile strength in each direction was investigated using the nozzle cutout pieces. As shown in Fig. 9, the difference in mechanical properties in the axial (A), tangential (T) and radial (R) directions was very small. Thus, the homogeneity of the forged shell ring was demonstrated.

As is apparent from the above-mentioned results of

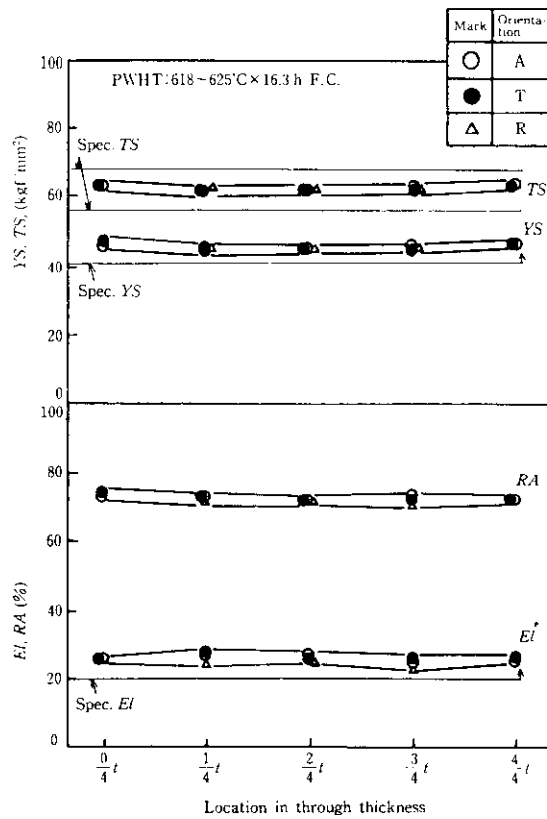


Fig. 9 Distribution of mechanical properties

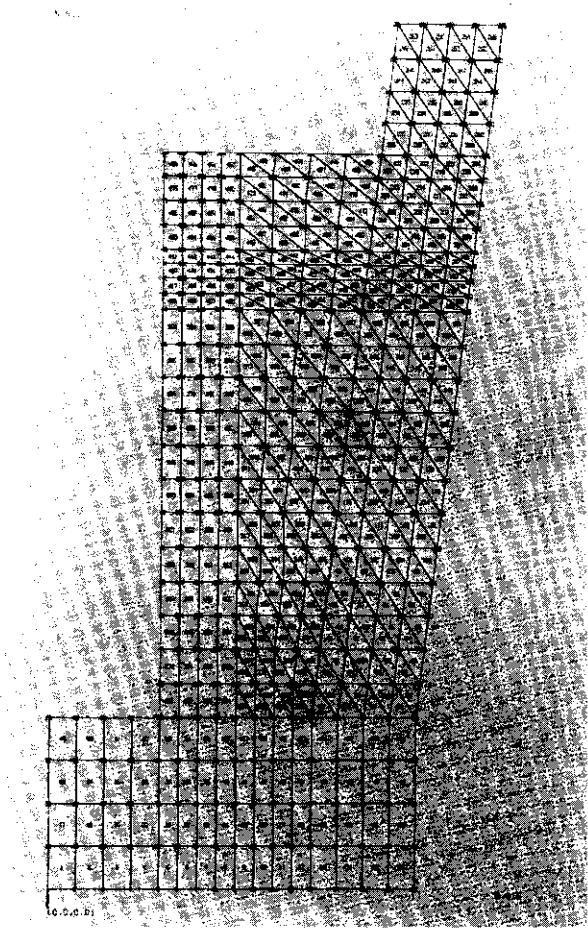


Fig. 10 Mesh divides of ingot and mould

investigations, it was found that the forged shell ring made from a hollow ingot shows only small changes in mechanical properties with position in the ingot due to the small segregation of the material, and is, moreover excellent in homogeneity.

4.2 Simulation of Solidification

The solidification process of ingots was predicted by computer simulation in order to ascertain the internal quality of hollow ingots used as the material for reactor pressure vessels. For this purpose, a fracture investigation of a 250-t ingot was conducted, and the correspondence between results of simulation and those of the fracture investigation was examined.

In the simulation of solidification, the following transient heat transfer equation was solved numerically by the direct differential method and a temperature field was determined.

$$C_p \rho \frac{\partial T}{\partial t} = \frac{\partial}{\partial x} \left(\lambda \frac{\partial T}{\partial x} \right) + \frac{\partial}{\partial y} \left(\lambda \frac{\partial T}{\partial y} \right) \dots \dots (2)$$

where T : Temperature
 t : Time
 C_p : Specific heat

ρ : Density

λ : Thermal conductivity

As shown in Fig. 10, the ingot and mold in this calculation were divided into about 1 000 meshes in forming a model. The heat transfer equation is differentiated as follows, by keeping a heat balance in the circum-center region for each node of the model thus obtained:

$$\rho C_p \frac{T'_i - T_i}{\Delta t} = \frac{1}{A_i} \sum_N \lambda \frac{D_{iN}}{R_{iN}} (t_N - t_i) \dots \dots (3)$$

where T'_i : Temperature after Δt time

A_i : Volume of circumcenter region

\sum_N : Sum for the nodes adjacent to node i

$D_{iN} R_{iN}$: Interface area and distance between nodes i and N

This difference equation was solved by using a computer. When this method is used, a solution can be obtained rapidly and with high accuracy, even with complicated shapes. Based on past results of temperature measurement, the heat transfer coefficients of natural air cooling, forced cooling, and mold cooling

(radiation heat transfer), each through a coating medium, were used as the boundary conditions for the top of the ingot, surface in contact with the core (inside diameter side), and surface in contact with the mold (outside diameter side), respectively.

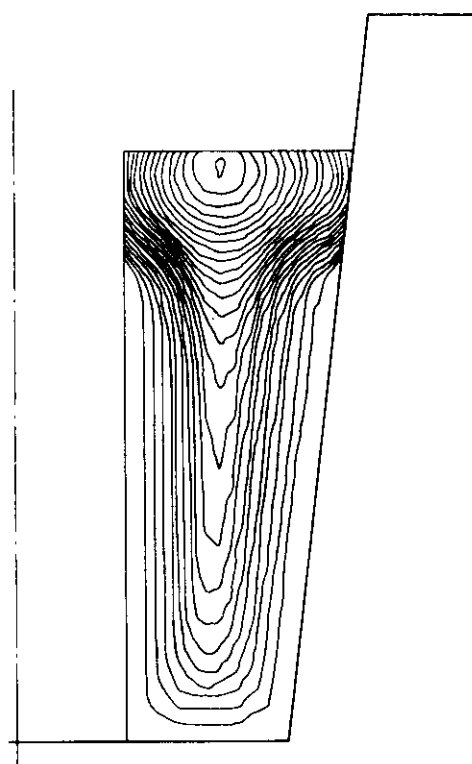


Fig. 11 Simulation result of solidification profile for 250 t hollow ingot

Results of the simulation of the solidification profile of the 250-t hollow ingot are shown in Fig. 11. These results are in good agreement with those shown in Photo 1. It was thus found that solidification proceeds gradually toward the center of the thickness due to cooling from both the core side and the mold side.

A comparison between prediction and results of the final solidification point in the inverted-V segregation region is shown in Fig. 12. Good agreement is observed between the two, showing it is possible to predict qualities of large ingots by simulation.

5 Conclusions

Kawasaki Steel manufactured a forged shell ring for a 1 300 MWe class nuclear reactor pressure vessel using a 220-t hollow ingot made by the basic oxygen furnace-RH degassing process. This product showed small segregation and a very clean internal surface. It was further demonstrated by a cross-sectional investigation of a 250-t hollow ingot that the hollow ingot is excellent in segregation and cleanliness, and meets manufacturing requirements even for very large upsized products.

Subsequently, on the basis of the results obtained, a forged shell ring for a 1 100 MWe class BWR pressure vessel was manufactured from a 320-t hollow ingot. This product was very homogeneous and fully displayed the advantages of hollow ingots. As a result of these findings, therefore, forged shell rings manufactured from hollow ingots made by the basic oxygen furnace-RH degassing process can be considered to be most suitable for use in reactor pressure vessels. The authors believe that fabricators can use these shell rings with complete confidence in response to the tendency toward adoption of forgings for nuclear applications.

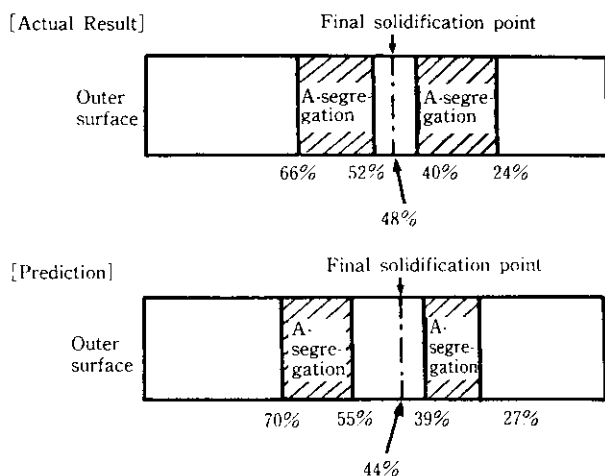


Fig. 12 Comparison of actual result and prediction concerning final solidification point and A-segregation

References

- 1) Japan Atomic Industry Committee: Table of Nuclear Power Station, (1984) 12
- 2) K. Kodaira: Nuclear Engineering (Genshiryoku Kogyo), 30(1984)5, 73
- 3) Y. Iida, T. Yamamoto, J. Matsuno, S. Yamaura, and K. Aso: "Manufacturing Process and Internal Quality of Large Ingots for Forgings", *Kawasaki Steel Giho*, 12(1980)1, 27
- 4) M. Ozawa, S. Okano, Y. Iida, T. Yamamoto, K. Aso, and N. Miyano: *Tetsu-to-Hagané*, 64(1978)11, S682
- 5) K. Aso, H. Wanaka, T. Yamamoto, M. Ozawa, and J. Matsuno: *Tetsu-to-Hagané*, 65(1979)4, S137
- 6) J. Nagai, M. Onishi, T. Yamamoto, A. Namba, R. Tachibana, and S. Kojima: "Producing High Quality Forging Ingots by LD-RH Process", *Kawasaki Steel Giho*, 15(1983)2, 66
- 7) M. Takada, H. Wanaka, K. Aso, Y. Arakawa, H. Mino, and A. Namba: "Outline of 4400 t Press and Manufacture of Large Forged Shell Rings", *Kawasaki Steel Giho*, 14(1982)4, 20
- 8) S. Koishi, S. Matsui, K. Aso, T. Watanabe, Y. Fukutaka: "New Manufacturing Process and Inspection Techniques of Large Forged Shell Ring", 3rd Japan-Deutch Seminar, Stuttgart, (1985)